



# Continuous fluorescence-based quantitative antioxidant assay using vegetable oil as an oxidizable substrate

Rajat Suhag<sup>a</sup>, Zongxin Jin<sup>b</sup>, Giovanna Ferrentino<sup>a</sup>, Riccardo Amorati<sup>b,\*</sup>, Matteo Scampicchio<sup>a</sup>

<sup>a</sup> Faculty of Agricultural, Environmental and Food Sciences, Free University of Bolzano, Piazza Università, 1, Bolzano 39100, Italy

<sup>b</sup> Department of Chemistry "G. Ciamician", University of Bologna, Via P. Gobetti 85, 40129 Bologna, Italy

## ARTICLE INFO

### Keywords:

Oxidation kinetics  
Inhibition  
Synergy  
Sunflower oil  
High-throughput  
Small-volume

## ABSTRACT

Several spectrophotometric assays, such as 1,1-diphenyl-2-picrylhydrazyl (DPPH) and oxygen radical absorbance capacity (ORAC), are commonly used to assess antioxidant activity. However, these methods often lack real-world relevance as they do not inhibit autoxidation in actual food substrates. Although direct measurement of oxygen consumption or peroxide formation during inhibited autoxidation offers certain advantages, it is labor intensive and requires specialized equipment. In this study, we introduce a small-volume inhibited autoxidation approach that utilizes a standard microplate reader and a food-derived oxidizable substrate, specifically stripped sunflower oil (SSO), and styrene-conjugated BODIPY (STY-BODIPY) chromophores that oxidizes with the substrate, enabling straightforward monitoring of the reaction progress without interfering with it. The rate of initiation ( $R_i$ ) was controlled by using azobis(isobutyronitrile) (AIBN) at 30 °C ( $R_i = 8.6 \pm 0.5 \times 10^{-10} \text{ M s}^{-1}$ ) to accurately determine the rate constant of antioxidant reaction with peroxy radicals ( $k_{\text{inh}}$ ). The method was standardized using the synthetic  $\alpha$ -tocopherol analogue 2,2,5,7,8-pentamethyl-6-chromanol (PMC) as a reference antioxidant and was successfully applied to evaluate its synergistic interactions with  $\gamma$ -terpinene, quercetin, and caffeic acid. The rate constant for the reaction of peroxy radicals with STY-BODIPY was determined,  $k_{\text{ST}} = 890 \pm 52 \text{ M}^{-1} \text{ s}^{-1}$ . Induction time ( $\tau$ ) of PMC increased in a concentration-dependent manner by the synergistic interactions of PMC/ $\gamma$ -terpinene, PMC/quercetin, and PMC/caffeic acid. The  $k_{\text{inh}}$  value for PMC in SSO at 30 °C remained constant at  $1.5 \times 10^6 \text{ M}^{-1} \text{ s}^{-1}$ . The validity of this approach was further confirmed using isothermal calorimetry, demonstrating its potential as a reliable and accessible tool for antioxidant testing in food systems.

## 1. Introduction

The increasing demand for simpler and more accessible approaches has driven the development of numerous assays for assessing "antioxidant activity" (Gulcin, 2020; Karagecili et al., 2023). Common examples include oxygen radical absorbance capacity (ORAC), cupric-ion reducing antioxidant capacity (CUPRAC), ferric reducing ability of plasma (FRAP), Folin-Ciocalteu's reagent reducing ability, scavenging effects in relation to 1,1-diphenyl-2-picrylhydrazyl (DPPH), and 2,2'-azino-bis(3-ethylbenzothiazoline-6-sulphonic acid) (ABTS) (Boyaci, Polat, & Kafkas, 2023; Fidan et al., 2020; Granato et al., 2018). These

methods typically rely on spectrophotometric techniques to determine the stoichiometry of the reaction between an antioxidant and an oxidizing agent with distinct absorbance properties. However, such assays do not involve peroxy radicals and are typically conducted in polar organic solvents devoid of an oxidizable substrate (Konopko & Litwinienko, 2022; Litwinienko & Ingold, 2007), whose protection from oxidation should represent the assay's actual end-point (Amorati & Valgimigli, 2018). Furthermore, when evaluating the antioxidant efficacy of a substance in preserving foods, it is essential to use an oxidizable substrate derived from food sources (Baschieri, Pizzol, Guo, Amorati, & Valgimigli, 2019; Laguerre, Lecomte, & Villeneuve, 2007).

**Abbreviations:** DPPH, 1,1-diphenyl-2-picrylhydrazyl; ORAC, oxygen radical absorbance capacity; SSO, stripped sunflower oil; STY-BODIPY, styrene-conjugated BODIPY (CAS 2383063-37-2); PMC, 2,2,5,7,8-pentamethyl-6-chromanol; CUPRAC, cupric-ion reducing antioxidant capacity; FRAP, ferric reducing ability of plasma; ABTS, 2,2'-azino-bis(3-ethylbenzothiazoline-6-sulfonic acid); GC-MS, gas chromatography-mass spectrometry; BHT, 2,6-di-*tert*-butyl-4-methylphenol; DPPH, diphenyl-1-picrylhydrazyl; THF, tetrahydrofuran; AIBN, 2,2'-azobis(isobutyronitrile); PMC/ $\gamma$ -terpinene, mixture of PMC +  $\gamma$ -terpinene; PMC/quercetin, mixture of PMC + quercetin; PMC/caffeic acid, mixture of PMC + caffeic acid.

\* Corresponding author.

E-mail address: [riccardo.amorati@unibo.it](mailto:riccardo.amorati@unibo.it) (R. Amorati).

<https://doi.org/10.1016/j.foodres.2024.115339>

Received 6 September 2024; Received in revised form 24 October 2024; Accepted 12 November 2024

Available online 17 November 2024

0963-9969/© 2024 The Author(s). Published by Elsevier Ltd. This is an open access article under the CC BY license (<http://creativecommons.org/licenses/by/4.0/>).

Considering that many of these assays also lack proper kinetic data analysis (Angeli, Morozova, & Scampicchio, 2023; Asma et al., 2024), the findings of existing spectrophotometric assays may have limited relevance to real food systems (Granato et al., 2018).

Autoxidation methods assess the ability of antioxidants to protect food-based substrates, such as triglycerides from vegetable oils from oxidative degradation. By using suitable kinetic analysis, these assays can offer valuable kinetic parameters that describe antioxidant action in real-time, such as the induction period length and the rate of oxidation in the presence or in the absence of an antioxidant (Baschieri et al., 2019; Guo, Pina, Gabbanini, & Valgimigli, 2024). Autoxidation of lipids can be monitored by measuring the amount of oxidized products. The detection of hydroperoxides can be performed via iodometric titration, or colorimetric assays that rely on the oxidation of  $\text{Fe}^{2+}$  to  $\text{Fe}^{3+}$  and the subsequent formation of colored iron salts. Conjugated dienes can be quantified by spectrophotometry, whereas volatile compounds, such as hexanal, are typically measured by gas chromatography-mass spectrometry (GC-MS) (Thomsen et al., 2016). However, these techniques are often susceptible to interferences and require discontinuous sampling and analysis. Oximetry is a well-established inhibited autoxidation technique that continuously measures the rate of oxygen consumption during lipid autoxidation. However, this approach is limited by low sensitivity and need for specialized instrumentation, which is often unavailable in many laboratories (Baschieri & Amorati, 2021). In addition, oximetry is constrained by low throughput, allowing only one sample to be analyzed at a time (Amorati, Baschieri, & Valgimigli, 2017).

To address these limitations, the introduction of a suitable fluorescent molecular probe into the system presents a practical solution for effectively monitoring the autoxidation process (Amorati & Valgimigli, 2018; Laguerre et al., 2007). Diphenyl-1-pyrenylphosphine (DPPP), which is non-fluorescent, reacts with lipid hydroperoxides to produce the DPPP = O oxide, a fluorescent compound with excitation and emission peaks at 351 and 380 nm, respectively (Mosca, Cuomo, Lopez, & Ceglie, 2013; Uluata, Durmaz, Julian McClements, & Decker, 2021). However, DPPP reacts slowly with hydroperoxides, making its application challenging in oxidation kinetics (Hanthorn, Haidasz, Gebhardt, & Pratt, 2012). BODIPY (4,4-difluoro-4-bora-3a,4a-diaza-s-indacene) dyes are small molecules with strong UV absorbance and sharp fluorescence emission peaks, with notable insensitivity to changes in the polarity and pH of the solvent and stability under physiological conditions (Brüls-Gill, Boerkamp, Hohlbein, & van Duynhoven, 2024; Yang et al., 2024). Among these, C11-BODIPY<sup>581/591</sup> is widely used for monitoring lipid oxidation (Kusio & Litwinienko, 2022), because of its susceptibility to oxidation in azo-initiated co-oxidation reactions with methyl linoleate (Yoshida, Shimakawa, Itoh, & Niki, 2003). The addition of the antioxidant BHT (2,6-di-*tert*-butyl-4-methylphenol) has been shown to inhibit this oxidation process. Pratt and co-workers further modified the C11-BODIPY<sup>581/591</sup> into the less oxidizable styrene-conjugated BODIPY (STY-BODIPY) for direct use in kinetic studies of the peroxidation of styrene, cumene, and tetrahydrofuran (THF) in the presence of an antioxidant (Haidasz, Van Kessel, & Pratt, 2016). These modifications allow for the determination of the inhibition rate constant of the reaction between the peroxy radicals and antioxidants ( $k_{inh}$ ) in competition with the reaction between the peroxy radical and the probe. These fluorescent probes are unique in that they co-participate in the propagation stage of the peroxidation process without interfering with the kinetic chain reaction (Haidasz et al., 2016).

Ideally, a method for determining antioxidant reactivity should combine the advantages of both traditional and inhibited autoxidation methods, specifically by being simple and rapid, utilizing standard laboratory equipment, using a food-derived oxidizable substrate, and providing accurate kinetic data for reactions between antioxidants and peroxy radicals. With this aim, we introduce a continuous fluorescence-based assay for quantitative antioxidant testing that monitor the reaction progress during inhibited autoxidation. This approach involves the

addition of a small amount of the fluorescent probe molecule STY-BODIPY to stripped sunflower oil (SSO), a food-based oxidizable substrate, allowing the reaction progress and its inhibition by antioxidants to be continuously monitored via fluorescence measurements in a 96-well microplate. The method is based on the competition between an antioxidant and a lipophilic, highly colored, and oxidizable fluorescent probe for peroxy radicals that propagate autoxidation. The methodology was standardized using the  $\alpha$ -tocopherol analogue 2,2,5,7,8-pentamethyl-6-chromanol (PMC) as a reference antioxidant in the co-oxidation of STY-BODIPY in SSO, as the inhibition rate constant ( $k_{inh}$ ) for PMC in sunflower oil is well-documented (Baschieri et al., 2019). The results were compared with those obtained by isothermal calorimetry, which we recently demonstrated to provide reliable autoxidation kinetics for studying antioxidants (Suhag et al., 2024). To evaluate the effectiveness of the STY-BODIPY co-oxidation method in addressing a relevant and compelling issue, synergistic interactions between PMC and various antioxidants were investigated (Bayram & Decker, 2024).

## 2. Materials and methods

### 2.1. Materials

Sodium hydroxide ( $\geq 97\%$ ), magnesium sulfate ( $\geq 99.5\%$ ), aluminum oxide (basic, activated), activated carbon, AIBN (2,2'-azobis(isobutyronitrile)) (98%), 2,2,5,7,8-pentamethyl-6-chromanol (PMC) (97%), quercetin ( $\geq 95\%$ ),  $\gamma$ -terpinene (97%), and caffeic acid ( $\geq 98.0\%$ ) were purchased from Sigma-Aldrich Chemical Co. (Milano, Italy).  $\gamma$ -terpinene was percolated twice through activated basic alumina and once through silica to remove impurities and hydroperoxide traces. Commercially available sunflower oil was obtained from a local market in Bolzano (Italy). Stripped sunflower oil was prepared by removing all naturally occurring antioxidants as described by Cui, McClements, and Decker (2015). Although STY-BODIPY is commercially available, it was synthesized by following a previously reported procedure (Haidasz et al., 2016) (see Supporting Information). All solvents and reagents were of analytical grade.

### 2.2. Co-oxidation of STY-BODIPY in stripped sunflower oil

To a 96-well black, flat bottom polystyrene plate (Costar®, Corning, USA), 130  $\mu\text{L}$  of stripped sunflower oil containing the azoinitiator AIBN, antioxidants and STY-BODIPY was added. After preliminary trials with various sample volumes, this sample volume was selected to ensure continuous oxygen diffusion, while maintaining a consistent oxidation rate. The plate was incubated at 30 °C in a microplate reader (Infinite M nano+, Tecan, Switzerland) with a shaking protocol (mode: linear and amplitude: 2 mm) for 5 min and a total incubation time of 15 min. STY-BODIPY in its reduced/native form emits a pseudo-red color; as chain-propagating peroxy radicals add to the styryl moiety forming non-conjugated products its fluorescence is shifted from 565 nm to 518 nm, exhibiting a green color (Fig. 1). The reaction progress was followed by monitoring the fluorescent oxidation product, STY-BODIPY<sub>ox</sub> ( $\lambda_{ex} = 488\text{ nm}$ ,  $\lambda_{em} = 518\text{ nm}$ ). The data were acquired by continuously reading the fluorescence from the top (detector gain: 70) at a 5 min time interval. Results were expressed as the concentration of STY-BODIPY<sub>ox</sub> by dividing the fluorescence data, expressed in relative fluorescence units (RFU), by a response factor of  $7.5 \times 10^4/\mu\text{M}$  STY-BODIPY, as shown in Eq. (1). The response factor was determined in turn by plotting the maximum fluorescence reached after complete consumption of the fluorescent probe as a function of STY-BODIPY concentration in SSO and was found to be in very good agreement with that reported for the co-oxidation of STY-BODIPY in phosphatidylcholine liposomes (Shah, Farmer, Zilka, Van Kessel, & Pratt, 2019).

$$[\text{STY-BODIPY}]_{\text{ox}} = \text{RFU}/75000 \quad (1)$$

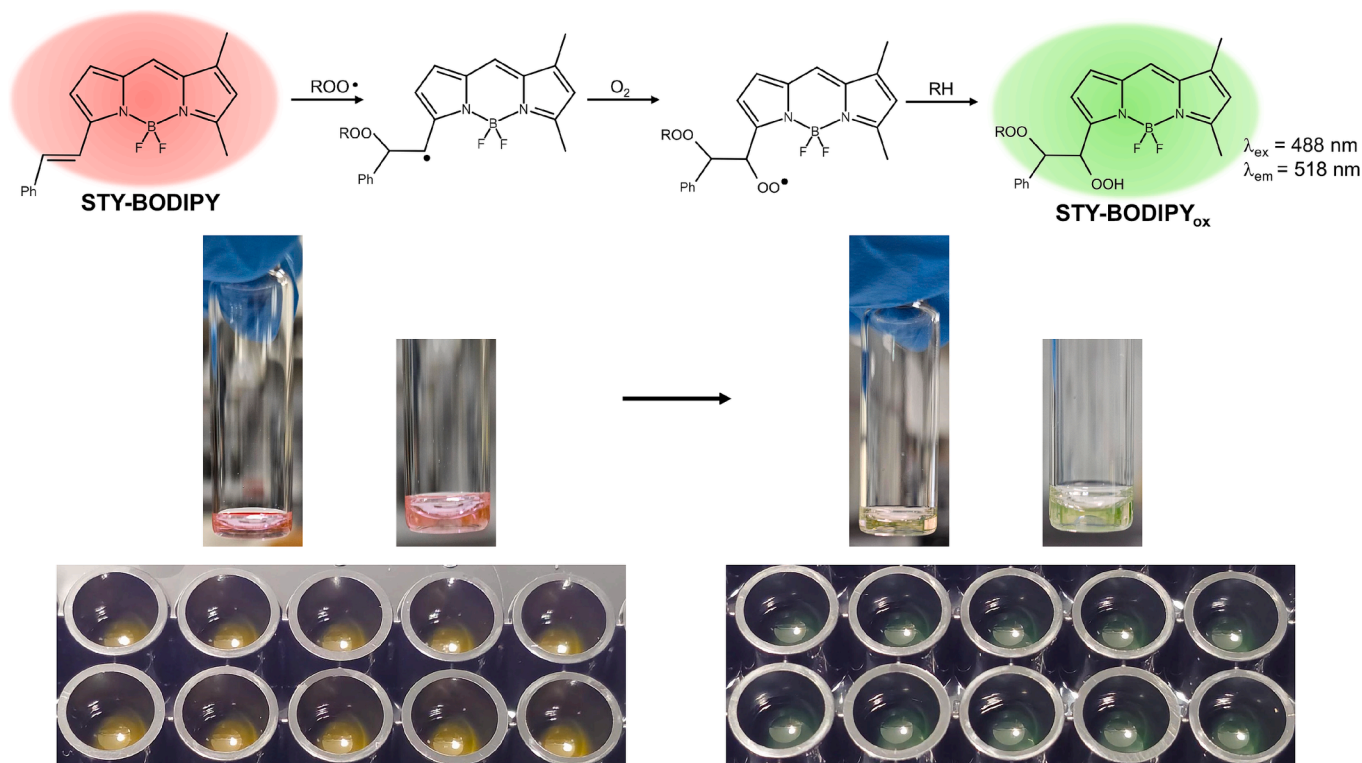


**Fig. 1.** Reaction of STY-BODIPY with peroxy radicals used as a signal carrier in co-oxidation with SSO and a visual representation of the color change of STY-BODIPY after reaction with peroxy radical to STY-BODIPY<sub>ox</sub> in a transparent vial and in a 96-well plate.

For a typical uninhibited co-oxidation experiment, SSO was added with AIBN (50 mM) and STY-BODIPY without any antioxidant, whereas the inhibited co-oxidation experiment contained PMC (3  $\mu\text{M}$ ) as a reference antioxidant. Furthermore, synergistic interactions were studied with PMC (3  $\mu\text{M}$ , fixed concentration) by adding different concentrations of  $\gamma$ -terpinene (6.3, 15.4 and 29.4 mM) – PMC/ $\gamma$ -terpinene, quercetin (3, 6, and 9  $\mu\text{M}$ ) – PMC/quercetin, and caffeic acid (10, 20 and 30  $\mu\text{M}$ ) – PMC/caffeic acid.

### 2.3. Co-oxidation kinetics

The kinetics of SSO co-oxidation in the presence of STY-BODIPY were analyzed by following the treatment proposed by Pratt and co-workers (Haidasz et al., 2016). Briefly, the rate of disappearance of the probe in the presence of the antioxidant ( $R_{\text{inh}}$ ) is given by Eq. (2), where  $k_{\text{ST}}$  is the rate constant for the reaction of  $\text{ROO}^\bullet$  radicals with STY-BODIPY,  $R_i$  is the rate of initiation due to AIBN decomposition, and  $n$  is the stoichiometry of radical-trapping (or the number of peroxy radicals trapped per molecule of antioxidant).

$$-R_{\text{inh}} = \frac{\delta[\text{STY-BODIPY}]_{\text{ox}}}{\delta t} = \frac{k_{\text{ST}}[\text{STY-BODIPY}]R_i}{nk_{\text{inh}}[\text{AH}]} \quad (2)$$

$$R_i = \frac{n[\text{AH}]}{\tau} \quad (3)$$

Under the reaction conditions, the amount of consumed AIBN was negligible, thus, the initiation rate,  $R_i$  is constant. The  $R_i$  value was determined using Eq. (3), with PMC as the reference antioxidant for which  $n = 2$  (Amorati et al., 2017).

### 2.4. Isothermal calorimetry

Isothermal calorimetry experiments were performed using a Thermal Activity Monitor (Model 421 TAM III, TA Instruments, Milan, Italy), a 24-channel microcalorimeter operating in isothermal mode. Glass

ampoules ( $4.0 \times 10^{-3}$  L) were accurately filled with 100 mg of stripped sunflower oil containing AIBN (50 mM) with (PMC alone, mixture of PMC/ $\gamma$ -terpinene and mixture of PMC/caffeic acid) and without antioxidants. The ampoules were maintained at a constant temperature (30 °C) in the dark inside the thermostat. Initially, a 15-min equilibration step was performed, during which the ampoule was held at mid-height inside the channel to establish temperature equilibrium between the sample and thermostat. The ampoule was then fully lowered into the measurement position during the experiment. Heat flow was recorded at 10-s intervals throughout the experiment.

### 2.5. Statistical analysis

Kinetic parameters including induction time ( $\tau$ ), stoichiometric factor ( $n$ ), and  $k_{\text{inh}}$  are expressed as the average  $\pm$  standard deviation (SD) from at least three independent kinetic measurements. One-way ANOVA followed by Tukey's post hoc test ( $p < 0.05$ ) was used to determine statistical significance. Figures showing the co-oxidation traces were prepared using OriginPro 2021 (version 9.8.0.200), OriginLab Corporation, USA.

## 3. Results and discussion

### 3.1. Standardization of STY-BODIPY co-oxidation in sunflower oil

To develop a robust model for quantitative antioxidant testing, stripped sunflower oil (SSO), a commercial oil depleted of its natural phenolic and carotenoid components, was used as an oxidizable substrate. The use of SSO was based on a previously established kinetic calibration (Baschieri et al., 2019). Fig. 2 shows the concentration profile of STY-BODIPY<sub>ox</sub> over time during the AIBN-initiated uninhibited and inhibited co-oxidation of STY-BODIPY (1  $\mu\text{M}$ ) in SSO at 30 °C. In the uninhibited co-oxidation, the concentration of STY-BODIPY<sub>ox</sub> increased linearly with time when SSO containing AIBN (50

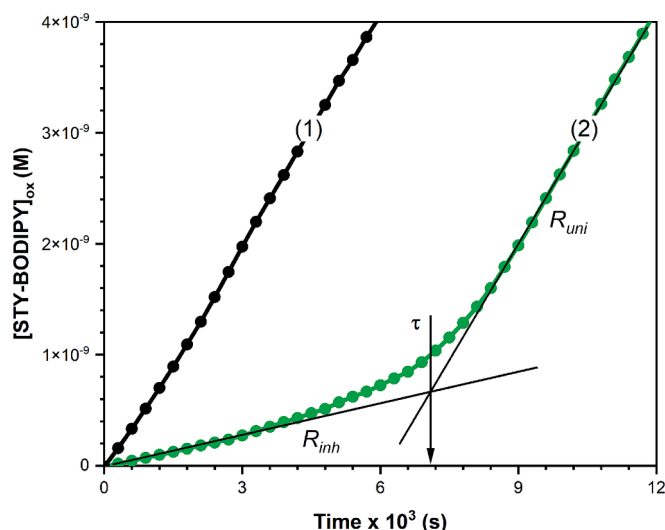


Fig. 2. Co-oxidation of STY-BODIPY in SSO, (1) initiated by AIBN (50 mM) and, (2) inhibited by PMC (3  $\mu\text{M}$ ).  $R_{inh}$ : rate of inhibited co-oxidation,  $R_{uni}$ : rate of uninhibited co-oxidation, and  $\tau$ : induction time.

mM) was used, indicating a steady progression of the oxidation.

For the inhibited co-oxidation experiments, PMC was selected as a reference antioxidant because of its well-characterized inhibition rate constant ( $k_{inh} = 1.5 \times 10^6 \text{ M}^{-1} \text{ s}^{-1}$ ) in SSO at 30 °C (Baschieri et al., 2019). The presence of PMC (3  $\mu\text{M}$ ), effectively slowed the oxidation process, as evidenced by a reduction in the rate of STY-BODIPY<sub>ox</sub> formation, resulting in an inhibited period shown in Fig. 2. The rate during this inhibited period, referred to as the rate of inhibition ( $R_{inh}$ ), serves as an indicator of the antioxidant efficacy in retarding oxidation. The duration of this inhibited period, known as the induction time ( $\tau$ ), indicates the point at which all effective antioxidants within the sample are completely consumed by radicals. The induction time is a critical parameter for assessing antioxidant, with longer  $\tau$  values indicating a greater antioxidant capacity (Guo, Baschieri, Amorati, & Valgimigli, 2021).

The autoxidation process was initiated with AIBN (50 mM) and the induction time was used to estimate the rate of initiation ( $R_i$ ), which was determined to be  $8.6 \pm 0.5 \times 10^{-10} \text{ M s}^{-1}$  (Eq. (3)) using PMC as a reference antioxidant with a known stoichiometry ( $n = 2$ ). Furthermore, the  $R_{inh}$  observed during the inhibited oxidation, together with  $R_i$  and the known  $k_{inh}$  for PMC (*vide supra*) allowed the determination of the rate constant for the reaction of peroxy radicals ( $\text{ROO}^\bullet$ ) with STY-BODIPY ( $k_{ST}$ ) using Eq. (2). The calculated value of  $k_{ST} = 890 \pm 52 \text{ M}^{-1} \text{ s}^{-1}$  closely aligns with the previously reported value of  $894 \text{ M}^{-1} \text{ s}^{-1}$  for STY-BODIPY by Shah et al. (2019), thereby confirming the validity of the experimental conditions and the fluorescence-based approach for kinetic antioxidant testing using a microplate reader and a food-derived oxidizable substrate.

After the induction time, the concentration of STY-BODIPY<sub>ox</sub> increased linearly, similar to the trend observed under uninhibited co-oxidation conditions, as depicted in Fig. 2.

### 3.2. Synergistic interaction of different antioxidants with PMC

To further validate the efficacy of our fluorescence-based assay for evaluating antioxidant activity, the synergistic interactions between PMC and various antioxidants were investigated. Specifically, we examined the well-documented synergistic interactions of  $\gamma$ -terpinene (Guo et al., 2021; Mollica, Gelabert, & Amorati, 2022), quercetin (Pedrielli & Skibsted, 2002; Zhang et al., 2023) and caffeic acid (Iglesias, Pazos, Andersen, Skibsted, & Medina, 2009) when combined with PMC.

The synergistic mechanism between PMC and quercetin or caffeic

acid involves a regeneration process. PMC acts as a chain-breaking antioxidant by donating hydrogen atoms to alkyl peroxy radicals, thereby forming a PMC radical, that subsequently traps another radical to form non-antioxidant products. Quercetin and caffeic acid can donate hydrogen atoms to PMC radicals, regenerating active PMC and producing quercetin quinone (Zhang et al., 2023). In contrast, the synergistic mechanism of  $\gamma$ -terpinene is based on the formation of hydroperoxy radicals ( $\text{HOO}^\bullet$ ) during its oxidation, which possess both reducing and oxidizing properties (Foti & Ingold, 2003). These radicals can donate a hydrogen atom to the PMC radical, restoring it to its original phenolic form (Guo et al., 2021). Due to this distinct mechanism,  $\gamma$ -terpinene is expected to be effective at relatively higher concentrations than quercetin and caffeic acid.

Fig. 3 (A) shows the concentration of STY-BODIPY<sub>ox</sub> over time during co-oxidation in the presence of  $\gamma$ -terpinene alone and in combination with PMC. The data show that  $\gamma$ -terpinene alone (Fig. 3 (A), trace (2)), even in the millimolar range, only slows the co-oxidation of STY-BODIPY in SSO without producing a clear induction time. However, the combination of PMC and  $\gamma$ -terpinene significantly ( $p < 0.05$ ) increased the induction time (Fig. 3 (A), trace 4) compared with PMC alone. Furthermore, testing various concentrations of  $\gamma$ -terpinene in combination with PMC revealed a linear relationship ( $R^2 = 0.99$ ) between the concentration of  $\gamma$ -terpinene and the induction time as shown in Fig. 3 (B). Table 1 presents the kinetic parameters derived from the co-oxidation of STY-BODIPY with SSO in the presence of PMC and the PMC/ $\gamma$ -terpinene combination. The apparent rate constant of inhibition ( $\text{app.}k_{inh}$ ) for the PMC/ $\gamma$ -terpinene mixture was similar to that of PMC alone ( $p > 0.05$ ). From the STY-BODIPY<sub>ox</sub> concentration vs. time plot, the apparent stoichiometry value ( $n$ ) for the PMC/ $\gamma$ -terpinene combination was calculated using Eq. (2). According to the well-established chain-breaking antioxidant mechanism, each molecule of phenol (PMC) neutralizes two  $\text{ROO}^\bullet$  radicals, resulting in  $n = 2$ . The apparent  $n$  values for the PMC/ $\gamma$ -terpinene combination were significantly ( $p < 0.05$ ) greater than 2, and increased with the concentration of  $\gamma$ -terpinene. This finding is consistent with previous oximetry studies at 30 °C and 130 °C, which attributed the higher  $n$  values to the reducing activity of  $\text{HOO}^\bullet$  radicals generated by  $\gamma$ -terpinene (Mollica et al., 2022).

Fig. 3(C) and (E), along with Table 1, show the results of the synergistic interaction between quercetin or caffeic acid and PMC. The addition of quercetin or caffeic acid at micromolar concentration, in combination with PMC, significantly ( $p < 0.05$ ) increased the induction time compared to PMC alone. Both antioxidants extended the induction time in a concentration-dependent manner, as shown in Fig. 3 (D) and (F), respectively. Furthermore, both quercetin and caffeic acid prolonged the induction time without altering the oxidation kinetics observed with PMC alone. These findings are consistent with previous studies on the synergistic activity of quercetin (Becker, Ntouma, & Skibsted, 2007; Nogala-Kalućka et al., 2013; Pedrielli & Skibsted, 2002; Zhang et al., 2023) and caffeic acid (Iglesias et al., 2009; Zhang et al., 2023) when combined with  $\alpha$ -tocopherol. Analysis of variance (ANOVA) showed a significant effect of the synergistic interactions of antioxidants on the induction time  $F(8,9) = 65.19$ ,  $p < 0.001$ ,  $\eta^2 = 0.983$  and stoichiometry factor  $F(8,9) = 62.24$ ,  $p < 0.001$ ,  $\eta^2 = 0.982$ .

The findings obtained from the continuous fluorescence-based approach were further corroborated by isothermal calorimetry analysis. Isothermal calorimetry, which continuously measures the heat flow of oxidation reactions, was previously validated by our group for studying the oxidation kinetics of oils (Mosibo, Laopeng, Ferrentino, & Scampicchio, 2022), emulsions (Suhag et al., 2024) and micro-encapsulated bioactive compounds (Klettenhammer et al., 2023). The synergistic activity of  $\gamma$ -terpinene and caffeic acid with PMC in SSO to inhibit AIBN initiated autoxidation at 30 °C was tested using isothermal calorimetry. Consistent with the fluorescence-based assay results, the induction time increased with the addition of both  $\gamma$ -terpinene and caffeic acid in concentration-dependent manner compared with PMC alone (Supplementary information Fig. S3).

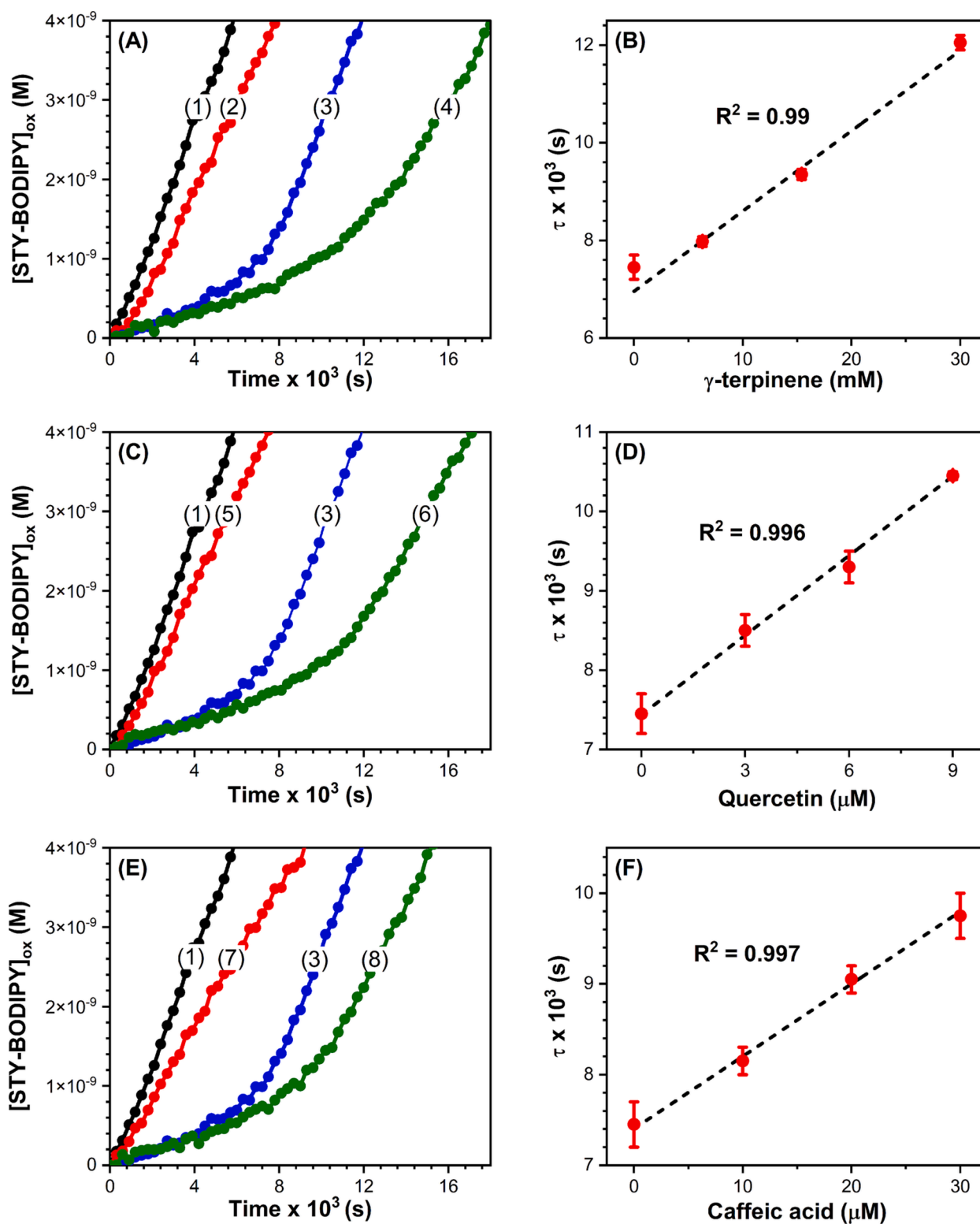


Fig. 3. Co-oxidation of STY-BODIPY in SSO initiated by AIBN (50 mM). In panels A, C, and E, trace 1: uninhibited co-oxidation, trace 2: inhibited by  $\gamma$ -terpinene, trace 3: inhibited by PMC, trace 4: inhibited by mixture of PMC/ $\gamma$ -terpinene, trace 5: inhibited by quercetin, trace 6: inhibited by mixture of PMC/quercetin, trace 7: inhibited by caffeic acid, and trace 8: inhibited by mixture of PMC/caffeic acid. Panels B, D, and F show the induction time ( $\tau$ ) vs the concentration of different mixtures of PMC/ $\gamma$ -terpinene, PMC/quercetin, and PMC/caffeic acid, respectively.

#### 4. Conclusion

This study introduced a simple and continuous quantitative method for assessing antioxidant activity based on inhibited autoxidation in

vegetable oil. By monitoring the fluorescence intensity of the STY-BODIPY probe during its co-oxidation in stripped sunflower oil, we tracked the reaction progress. The method was calibrated using PMC as a reference antioxidant and could successfully determine its synergistic

**Table 1**

Kinetic parameters of mixture of PMC with different antioxidants during the co-oxidation of STY-BODIPY with stripped sunflower oil added with 50 mM AIBN at 30 °C.

Antioxidant	Concentration	$\tau$ ( $10^3$ s)	$n$	app. $k_{inh}$ ( $10^6$ $M^{-1} s^{-1}$ )
PMC	3 $\mu$ M	7.5 $\pm$ 0.2	2.0	1.5
PMC + $\gamma$ -terpinene	3 $\mu$ M+6.3 mM	8.0 $\pm$ 0.1 <sup>e</sup>	2.3 $\pm$ 0.1 <sup>e</sup>	1.2 $\pm$ 0.3 <sup>a</sup>
	3 $\mu$ M+15.4 mM	9.4 $\pm$ 0.1 <sup>cd</sup>	2.7 $\pm$ 0.1 <sup>cd</sup>	1.3 $\pm$ 0.1 <sup>a</sup>
	3 $\mu$ M+29.4 mM	12.1 $\pm$ 0.2 <sup>a</sup>	3.3 $\pm$ 0.3 <sup>a</sup>	1.2 $\pm$ 0.2 <sup>a</sup>
PMC + quercetin	3 $\mu$ M+3 $\mu$ M	8.5 $\pm$ 0.2 <sup>de</sup>	2.4 $\pm$ 0.1 <sup>de</sup>	1.1 $\pm$ 0.3 <sup>a</sup>
	3 $\mu$ M+6 $\mu$ M	9.3 $\pm$ 0.2 <sup>cd</sup>	2.7 $\pm$ 0.2 <sup>cd</sup>	1.2 $\pm$ 0.2 <sup>a</sup>
	3 $\mu$ M+9 $\mu$ M	10.5 $\pm$ 0.2 <sup>b</sup>	3.0 $\pm$ 0.2 <sup>b</sup>	1.2 $\pm$ 0.1 <sup>a</sup>
PMC + caffeic acid	3 $\mu$ M+10 $\mu$ M	8.2 $\pm$ 0.1 <sup>e</sup>	2.3 $\pm$ 0.2 <sup>e</sup>	1.3 $\pm$ 0.3 <sup>a</sup>
	3 $\mu$ M+20 $\mu$ M	9.1 $\pm$ 0.2 <sup>cd</sup>	2.6 $\pm$ 0.1 <sup>cd</sup>	1.2 $\pm$ 0.2 <sup>a</sup>
	3 $\mu$ M+30 $\mu$ M	9.8 $\pm$ 0.3 <sup>bc</sup>	2.8 $\pm$ 0.2 <sup>bc</sup>	1.1 $\pm$ 0.3 <sup>a</sup>

Mean  $\pm$  SD that do not share a superscript letter are significantly different ( $p < 0.05$ ).  $\tau$ : induction time,  $n$ : stoichiometry factor, app. $k_{inh}$ : rate constant of inhibition reaction for the mixture of antioxidants. The  $n$  and  $k_{inh}$  data for PMC are from literature (Baschieri et al., 2019).

interactions with  $\gamma$ -terpinene, quercetin, and caffeic acid. A key advantage of this approach is the use of a microplate, which enabled the simultaneous analysis of multiple samples, resulting in a high-throughput method. This setup minimizes variability and enhances the robustness of the findings by allowing all samples to be processed under identical conditions. It is particularly beneficial in kinetic studies, where real-time monitoring of multiple samples improves precision. Furthermore, the reduced sample volume required per well makes this method more cost-effective and efficient compared to single-cell fluorimeters, which typically require larger volumes and individual processing. However, for laboratories lacking access to this equipment, adaptations using single-sample fluorimeters with temperature control can still yield similar results, although they may result in lower throughput and increased hands-on time. Future studies will address the use of different food-relevant oxidizable materials (i.e. emulsions, gels), and initiation strategies (i.e. heat, metals, peroxides).

#### CRediT authorship contribution statement

**Rajat Suhag:** Writing – original draft, Methodology, Investigation, Formal analysis, Data curation, Conceptualization. **Zongxin Jin:** Writing – original draft, Investigation, Data curation. **Giovanna Ferrantino:** Writing – review & editing, Investigation, Data curation. **Riccardo Amorati:** Writing – review & editing, Visualization, Supervision, Funding acquisition, Formal analysis, Conceptualization. **Matteo Scampicchio:** Writing – review & editing, Supervision, Funding acquisition, Formal analysis, Conceptualization.

#### Declaration of competing interest

The authors declare the following financial interests/personal relationships which may be considered as potential competing interests: Matteo Scampicchio reports financial support was provided by Italian Ministry of University and Research and by VOG Products (project code P211).

#### Acknowledgements

The authors would like to thank VOG Products company for the financial support. They would like also to acknowledge the support by the China Scholarship Council (CSC: 202209120002), the European Union - NextGenerationEU under the National Recovery and Resilience Plan (PNRR) – Mission 4 Education and research – Component 2 From research to business – Investment 1.1 Notice Prin 2022 – DD N. 104 del 2/2/2022, from PRIN20227XZKBY – Superoxide responsive redox-active systems and nano smart materials to target ferroptosis – FEROX – CUP J53D23008550006”.

#### Appendix A. Supplementary data

Supplementary data to this article can be found online at <https://doi.org/10.1016/j.foodres.2024.115339>.

#### Data availability

Data will be made available on request.

#### References

- Amorati, R., Baschieri, A., & Valgimigli, L. (2017). Measuring antioxidant activity in bioorganic samples by the differential oxygen uptake apparatus: Recent advances. *Journal of Chemistry*, 2017, 1–12. <https://doi.org/10.1155/2017/6369358>
- Amorati, R., & Valgimigli, L. (2018). Methods to measure the antioxidant activity of phytochemicals and plant extracts. *Journal of Agricultural and Food Chemistry*, 66(13), 3324–3329. <https://doi.org/10.1021/acs.jafc.8b01079>
- Angeli, L., Morozova, K., & Scampicchio, M. (2023). A kinetic-based stopped-flow DPPH• method. *Scientific Reports*, 13(1). <https://doi.org/10.1038/S41598-023-34382-7>
- Asma, U., Bertotti, M. L., Zamai, S., Arnold, M., Amorati, R., & Scampicchio, M. (2024). A kinetic approach to Oxygen Radical Absorbance Capacity (ORAC): Restoring order to the antioxidant activity of hydroxycinnamic acids and fruit juices. *Antioxidants*, 13(2), 222. <https://doi.org/10.3390/antiox13020222>
- Baschieri, A., & Amorati, R. (2021). Methods to determine chain-breaking antioxidant activity of nanomaterials beyond DPPH•. A review. *Antioxidants*, 10(10), 1551. <https://doi.org/10.3390/antiox10101551>
- Baschieri, A., Pizzol, R., Guo, Y., Amorati, R., & Valgimigli, L. (2019). Calibration of squalene, p-cymene, and sunflower oil as standard oxidizable substrates for quantitative antioxidant testing. *Journal of Agricultural and Food Chemistry*, 67(24), 6902–6910. <https://doi.org/10.1021/acs.jafc.9b01400>
- Bayram, L., & Decker, E. A. (2024). Analysis of the mechanism of antioxidant synergism between  $\alpha$ -tocopherol and myricetin in bulk oil. *Journal of the American Oil Chemists' Society*, 101(5), 477–492. <https://doi.org/10.1002/aocs.12792>
- Becker, E. M., Ntouma, G., & Skibsted, L. H. (2007). Synergism and antagonism between quercetin and other chain-breaking antioxidants in lipid systems of increasing structural organisation. *Food Chemistry*, 103(4), 1288–1296. <https://doi.org/10.1016/j.foodchem.2006.10.034>
- Boyaci, S., Polat, S., & Kafkas, N. E. (2023). Determination of the phytochemical contents and pomological properties of chokeberry (*Aronia melanocarpa* L.) fruit in different harvesting periods. *Turkish Journal of Agriculture and Forestry*, 47(6), 842–850. <https://doi.org/10.55730/1300-011X.3132>
- Brüls-Gill, M., Boerkamp, V. J. P., Hohlbein, J., & van Duynhoven, J. P. M. (2024). Spatiotemporal assessment of protein and lipid oxidation in concentrated oil-in-water emulsions stabilized with legume protein isolates. *Current Research in Food Science*, 9, Article 100817. <https://doi.org/10.1016/j.crfs.2024.100817>
- Cui, L., McClements, D. J., & Decker, E. A. (2015). Impact of phosphatidylethanolamine on the antioxidant activity of  $\alpha$ -tocopherol and trolox in bulk oil. *Journal of Agricultural and Food Chemistry*, 63(12), 3288–3294. <https://doi.org/10.1021/acs.jafc.5b00243>
- Fidan, H., Stankov, S., Petkova, N., Petkova, Z., Iliev, A., Stoyanova, M., Ivanova, T., Zhelyazkov, N., Ibrahim, S., Stoyanova, A., & Ercisli, S. (2020). Evaluation of chemical composition, antioxidant potential and functional properties of carob (*Ceratonia siliqua* L.) seeds. *Journal of Food Science and Technology*, 57(7), 2404–2413. <https://doi.org/10.1007/s13197-020-04274-z>
- Foti, M. C., & Ingold, K. U. (2003). Mechanism of inhibition of lipid peroxidation by  $\gamma$ -terpinene, an unusual and potentially useful hydrocarbon antioxidant. *Journal of Agricultural and Food Chemistry*, 51(9), 2758–2765. <https://doi.org/10.1021/jf020993f>
- Granato, D., Shahidi, F., Wrolstad, R., Kilmartin, P., Melton, L. D., Hidalgo, F. J., Miyashita, K., van Camp, J., Alasalvar, C., Ismail, A. B., Elmore, S., Birch, G. G., Charalampopoulos, D., Astley, S. B., Pegg, R., Zhou, P., & Finglas, P. (2018). Antioxidant activity, total phenolics and flavonoids contents: Should we ban in vitro screening methods? *Food Chemistry*, 264, 471–475. <https://doi.org/10.1016/j.foodchem.2018.04.012>
- Gulcin, İ. (2020). Antioxidants and antioxidant methods: An updated overview. *Archives of Toxicology*, 94(3), 651–715. <https://doi.org/10.1007/s00204-020-02689-3>

- Guo, Y., Baschieri, A., Amorati, R., & Valgimigli, L. (2021). Synergic antioxidant activity of  $\gamma$ -terpinene with phenols and polyphenols enabled by hydroperoxyl radicals. *Food Chemistry*, 345, Article 128468. <https://doi.org/10.1016/j.foodchem.2020.128468>
- Guo, Y., Pina, A., Gabbanini, S., & Valgimigli, L. (2024). Absolute kinetics of peroxidation and antioxidant protection of intact triglyceride vegetable oils. *Food Chemistry*, 452, Article 139289. <https://doi.org/10.1016/j.foodchem.2024.139289>
- Haidasz, E. A., Van Kessel, A. T. M., & Pratt, D. A. (2016). A continuous visible light spectrophotometric approach to accurately determine the reactivity of radical-trapping antioxidants. *The Journal of Organic Chemistry*, 81(3), 737–744. <https://doi.org/10.1021/acs.joc.5b02183>
- Hanthorn, J. J., Haidasz, E., Gebhardt, P., & Pratt, D. A. (2012). A versatile fluorescence approach to kinetic studies of hydrocarbon autoxidations and their inhibition by radical-trapping antioxidants. *Chemical Communications*, 48(81), 10141. <https://doi.org/10.1039/c2cc35214a>
- Iglesias, J., Pazos, M., Andersen, M. L., Skibsted, L. H., & Medina, I. (2009). Caffeic acid as antioxidant in fish muscle: Mechanism of synergism with endogenous ascorbic acid and  $\alpha$ -tocopherol. *Journal of Agricultural and Food Chemistry*, 57(2), 675–681. <https://doi.org/10.1021/jf802888w>
- Karagecili, H., Yilmaz, M. A., Ertürk, A., Kiziltas, H., Güven, L., Alwasel, S. H., & Gulcin, İ. (2023). Comprehensive metabolite profiling of berdav propolis using LC-MS/MS: Determination of antioxidant, anticholinergic, antiglaucoma, and antidiabetic effects. *Molecules*, 28(4), 1739. <https://doi.org/10.3390/molecules28041739>
- Klettenhammer, S., Ferrentino, G., Imperiale, S., Segato, J., Morozova, K., & Scampicchio, M. (2023). Oxidative stability by isothermal calorimetry of solid lipid microparticles produced by particles from gas saturated solutions technique. *LWT*, 173, Article 114370. <https://doi.org/10.1016/j.lwt.2022.114370>
- Konopko, A., & Litwinienko, G. (2022). Mutual activation of two radical trapping agents: Unusual “Win–Win Synergy” of resveratrol and TEMPO during scavenging of dpph • radical in methanol. *The Journal of Organic Chemistry*, 87(22), 15530–15538. <https://doi.org/10.1021/acs.joc.2c02080>
- Kusio, J., & Litwinienko, G. (2022). *Fluorescent Probes for Monitoring Oxidation of Lipids and Assessment of Antioxidant Activity*. In *Lipid Oxidation in Food and Biological Systems* (pp. 49–91). Springer International Publishing. [https://doi.org/10.1007/978-3-030-87222-9\\_3](https://doi.org/10.1007/978-3-030-87222-9_3)
- Laguerre, M., Lecomte, J., & Villeneuve, P. (2007). Evaluation of the ability of antioxidants to counteract lipid oxidation: Existing methods, new trends and challenges. *Progress in Lipid Research*, 46(5), 244–282. <https://doi.org/10.1016/j.plipres.2007.05.002>
- Litwinienko, G., & Ingold, K. U. (2007). Solvent effects on the rates and mechanisms of reaction of phenols with free radicals. *Accounts of Chemical Research*, 40(3), 222–230. <https://doi.org/10.1021/ar0682029>
- Mollica, F., Gelabert, I., & Amorati, R. (2022). Synergic antioxidant effects of the essential oil component  $\gamma$ -terpinene on high-temperature oil oxidation. *ACS Food Science & Technology*, 2(1), 180–186. <https://doi.org/10.1021/acscfoodscitech.1c00399>
- Mosca, M., Cuomo, F., Lopez, F., & Ceglie, A. (2013). Role of emulsifier layer, antioxidants and radical initiators in the oxidation of olive oil-in-water emulsions. *Food Research International*, 50(1), 377–383. <https://doi.org/10.1016/j.foodres.2012.10.046>
- Mosibo, O. K., Laopeng, S., Ferrentino, G., & Scampicchio, M. (2022). Oxidizability of oils recovered from olive seeds by isothermal calorimetry. *Foods*, 11(7), 1016. <https://doi.org/10.3390/foods11071016>
- Nogala-Kalućka, M., Dwiecki, K., Siger, A., Górnica{acute{s}}, P., Polewski, K., & Ciosek, S. (2013). Antioxidant synergism and antagonism between tocotrienols, quercetin and rutin in model system. *Acta Alimentaria*, 42(3), 360–370. <https://doi.org/10.1556/AAlim.2012.0009>
- Pedrielli, P., & Skibsted, L. H. (2002). Antioxidant synergy and regeneration effect of quercetin, (–)-epicatechin, and (+)-catechin on  $\alpha$ -tocopherol in homogeneous solutions of peroxidating methyl linoleate. *Journal of Agricultural and Food Chemistry*, 50(24), 7138–7144. <https://doi.org/10.1021/jf0204371>
- Shah, R., Farmer, L. A., Zilka, O., Van Kessel, A. T. M., & Pratt, D. A. (2019). Beyond DPPH: Use of fluorescence-enabled inhibited autoxidation to predict oxidative cell death rescue. *Cell Chemical Biology*, 26(11), 1594–1607.e7. <https://doi.org/10.1016/j.chembiol.2019.09.007>
- Suhag, R., Ferrentino, G., Morozova, K., Zatelli, D., Scampicchio, M., & Amorati, R. (2024). Antioxidant efficiency and oxidizability of mayonnaise by oximetry and isothermal calorimetry. *Food Chemistry*, 433, Article 137274. <https://doi.org/10.1016/j.foodchem.2023.137274>
- Thomsen, B. R., Yesiltas, B., Sørensen, A. M., Hermund, D. B., Glastrup, J., & Jacobsen, C. (2016). Comparison of three methods for extraction of volatile lipid oxidation products from food matrices for GC–MS analysis. *Journal of the American Oil Chemists' Society*, 93(7), 929–942. <https://doi.org/10.1007/s11746-016-2837-2>
- Uluata, S., Durmaz, G., Julian McClements, D., & Decker, E. A. (2021). Comparing DPPP fluorescence and UV based methods to assess oxidation degree of krill oil-in-water emulsions. *Food Chemistry*, 339, Article 127898. <https://doi.org/10.1016/j.foodchem.2020.127898>
- Yang, S., ten Klooster, S., Nguyen, K. A., Hennebelle, M., Berton-Carabin, C., Schroën, K., van Duynhoven, J. P. M., & Hohlbein, J. (2024). Droplet size dependency and spatial heterogeneity of lipid oxidation in whey protein isolate-stabilized emulsions. *Food Research International*, 188, Article 114341. <https://doi.org/10.1016/j.foodres.2024.114341>
- Yoshida, Y., Shimakawa, S., Itoh, N., & Niki, E. (2003). Action of DCFH and BODIPY as a probe for radical oxidation in hydrophilic and lipophilic domain. *Free Radical Research*, 37(8), 861–872. <https://doi.org/10.1080/1071576031000148736>
- Zhang, Y., Wang, X., Zeng, Q., Deng, Y., Xie, P., Zhang, C., & Huang, L. (2023). A new insight into synergistic effects between endogenous phenolic compounds additive and  $\alpha$ -tocopherol for the stability of olive oil. *Food Chemistry*, 427, Article 136667. <https://doi.org/10.1016/j.foodchem.2023.136667>